# Inactivation as a New Regulatory Mechanism for Neuronal Kv7 Channels

Henrik Sindal Jensen,*‡ Morten Grunnet,*† and Søren-Peter Olesen*†
*The Danish National Research Foundation Centre for Cardiac Arrhythmia, Department of Medical Physiology, The Panum Institute, University of Copenhagen, DK-2200 Copenhagen N, Denmark; †NeuroSearch A/S, Ballerup, Denmark; and ‡H. Lundbeck A/S, Copenhagen, Denmark

ABSTRACT Voltage-gated $K^+$ channels of the Kv7 (KCNQ) family have important physiological functions in both excitable and nonexcitable tissue. The family encompasses five genes encoding the channel subunits Kv7.1–5. Kv7.1 is found in epithelial and cardiac tissue. Kv7.2–5 channels are predominantly neuronal channels and are important for controlling excitability. Kv7.1 channels have been considered the only Kv7 channels to undergo inactivation upon depolarization. However, here we demonstrate that inactivation is also an intrinsic property of Kv7.4 and Kv7.5 channels, which inactivate to a larger extent than Kv7.1 channels at all potentials. We demonstrate that at least 30% of these channels are inactivated at physiologically relevant potentials. The onset of inactivation is voltage dependent and occurs on the order of seconds. Both time- and voltage-dependent recovery from inactivation was investigated for Kv7.4 channels. A time constant of 1.47 ± 0.21 s and a voltage constant of 54.9 ± 3.4 mV were determined. It was further demonstrated that heteromeric Kv7.3/Kv7.4 channels had inactivation properties different from homomeric Kv7.4 channels. Finally, the Kv7 channel activator BMS-204352 was in contrast to retigabine found to abolish inactivation of Kv7.4. In conclusion, this work demonstrates that inactivation is a key regulatory mechanism of Kv7.4 and Kv7.5 channels.

## INTRODUCTION

The Kv7 family of ion channels has received much attention since they have been identified as the molecular correlates of several important human $K^+$ conductances. The Kv7 family is unique in the sense that mutations in four of the five genes have been linked to human hereditary diseases (1,2). Within the Kv7 family the most thorough characterization has been performed on the Kv7.1 channel (for a recent review see Jespersen et al. (3)). It was cloned in 1996 from patients suffering from the proarrhythmic condition long QT syndrome (4) and later demonstrated to associate with the $\beta$-subunits KCNE1 to constitute the cardiac $I_{Ks}$ current (5,6).

The neuronal M-current was first described in 1980 as slowly activating, noninactivating $K^+$ current, which could be inhibited through activation of muscarinic receptors (7). The molecular component behind the M-current was later identified as Kv7.2 and Kv7.3, and it has been demonstrated how mutations in these genes are linked to a neonatal form of epilepsy (8–12). Kv7.4 was cloned in 1999 and mutations in this gene have been associated with deafness (13–15). Kv7.5, like Kv7.2–4, is primarily neuronal, although no disease has yet been associated to mutations in this gene (16–18).

Due to the tight coupling of Kv7 channels to dysfunction and disease, great effort has been invested to understand the regulation of these channels. Kv7.1 channels are modulated by a number of factors including protein kinase A (PKA) and protein kinase C (PKC), cell volume changes, external acidification, and phosphatidyl inositol phosphate ($PIP_2$) (19–24). Additionally, Kv7.1 channel activity can be regulated by interaction with all members of the KCNE family of $\beta$-subunits (5,6,25–28).

As the molecular correlates of the M-current, Kv7.2 and Kv7.3 can be inhibited via muscarinic M1 receptor activation, although inhibition of the M-current can also be achieved through activation of other G-protein coupled receptors (29–31). $PIP_2$ has been demonstrated to be the link between muscarinic receptors and the M-current (32–35), and it is necessary for maintaining channel activity. Kv7.4 channels are regulated by factors such as PKA, PKC, intracellular $Ca^{2+}$, changes in cell volume, $PIP_2$, and phosphorylation by glucocorticoid-inducible kinases (19,36,37). Finally, changes in cell volume, extracellular $Zn^{2+}$, acidification, and muscarinic receptor activation modulate Kv7.5 (16,17). In addition to the described regulations, Kv7 channel activation is voltage dependent. A common feature is an initial opening at potentials around −60 mV and a slow time constant for both activation and deactivation compared to other voltage-gated $K^+$ channels.

One biophysical parameter that differentiates the Kv7 channel subtypes is inactivation. Inactivation has been reported for Kv7.1 channels and has been demonstrated to be time and voltage dependent (5,6). Coassembly with either KCNE1 or KCNE4 $\beta$-subunits can eliminate Kv7.1 channel inactivation (38–40). In contrast, it is generally believed that Kv7.2-5 channels—along with the M-current—do not inactivate (7,11, 13,17,18,39). However, a recent report shows that the activity of Kv7.4 channels can be augmented by hyperpolarizing prepulses, indicating that they may undergo inactivation (37). We have devoted this study to a thorough investigation of the

*Submitted November 16, 2006, and accepted for publication January 4, 2007.*

Address reprint requests to Henrik Sindal Jensen, Dept. of Molecular and Cellular Pharmacology, H. Lundbeck A/S, Ottiliavej 9, DK-2500 Copenhagen, Denmark. Tel.: 45-36-43-26-23; Fax: 45-36-43-82-71; E-mail: hsin@lundbeck.com.



0006-3495/07/04/2747/10 $2.00

doi: 10.1529/biophysj.106.101287

possible inactivation properties of all the Kv7 channels with emphasis on Kv7.4 channels.

## MATERIALS AND METHODS

### Molecular biology

cRNA was synthesized by standard T7 in vitro run-off transcription of human Kv7.1, Kv7.2, Kv7.3, and Kv7.4 and murine Kv7.5. A total of 50 nl of ~0.5 $\mu$g/$\mu$l cRNA was injected into stage V–VI oocytes isolated from *Xenopus laevis* according to national guidelines. Oocytes were kept at 19°C in Kulori solution (in mM: 90 NaCl, 1 KCl, 1 $MgCl_2$, 1 $CaCl_2$, 5 HEPES, pH 7.4) and currents could be detected after 2–3 days.

### Electrophysiology

Conventional two-electrode voltage-clamp recordings were conducted at room temperature in Kulori solution using a Dagan CA-1D amplifier (Minneapolis, MN) and Pulse software (HEKA, Lambrecht/Pfalz, Germany). The borosilicate electrodes were filled with 1 M KCl and had a tip resistance of 0.5–2 M$\Omega$. All drugs were dissolved in dimethylsulfoxide (DMSO) and diluted so the final DMSO concentration was <0.3%. At this concentration no vehicle effects were observed. Retigabine, BMS-204352, and XE-991 were synthesized at NeuroSearch A/S.

### Calculations

Data were obtained from more than one batch of oocytes, and analyses were performed in SigmaPlot. Data analyses were done with the Marquardt-Levenberg algorithm, and decaying currents were best fitted to a three-parameter single exponential function: $I(x) = A_\infty + A \times \exp(-x/\tau)$. Rising currents were best fitted to a three-parameter single exponential function: $I(x) = A_0 + A \times (1 - \exp(-x/\tau))$. For both equations $I(x)$ is the current at time or voltage $x$, $A$ is the amplitudes of the exponential, and $\tau$ is the time or voltage constant. For functions describing an exponential decline $A_\infty$ is the horizontal asymptotic value at time $\infty$, and for those describing an exponential rise $A_0$ is the current amplitude at time 0. The percentage of control are calculated as the $I_x/I_{CTRL} \times 100\%$, where $I_x$ is the normalized current amplitude after retigabine, XE-991, or BMS-204352 application and $I_{CTRL}$ is the corresponding current amplitude recorded in Kulori solution. Normalization is done to the current amplitude recorded at $V_{act} = +40$ mV after a $V_{pre}$ of $-120$ mV. The linear curve fits on the percentage of control data for the pharmacological experiments are fitted to $p(x) = \alpha x + \beta$, where $p(x)$ is the percentage of control at potential $x$, $\alpha$ is the slope, and $\beta$ the crossover point of $x = 0$. Values are given as mean ± SE where $n$ indicates the number of observations, and the mean is calculated as the mean of the particular parameter from several individual fits.

## RESULTS

### Inactivation properties of homomeric Kv7.1-5 channels

The extent of inactivation of homomeric Kv7.1, 2, 4, and 5 channels was investigated by two-electrode voltage clamp experiments in *Xenopus* oocytes. After injection of the respective cRNAs, typical Kv7 currents could be activated by standard voltage-step protocols consisting of a 3-s prepulse at $-80$ mV ($V_{pre}$), a 2-s activation pulse at gradually more positive potentials from $-100$ to $+60$ mV in 20-mV increments to activate the channels ($V_{act}$), and ended by a 1-s step to $-30$ mV to facilitate recording of the tail current (Fig. 1, *A–D*). Water-injected control oocytes did not give rise to interfering currents. From such experiments, the inactivation of the Kv7 channels is normally not visible, although indication of an inactivation process can be seen from a small hook on the tail current indicative of a release from inactivation (e.g., Fig. 1, *A* and *D*).

To study this phenomenon in more detail, we designed the inactivation protocol shown in Fig. 2 with an initial

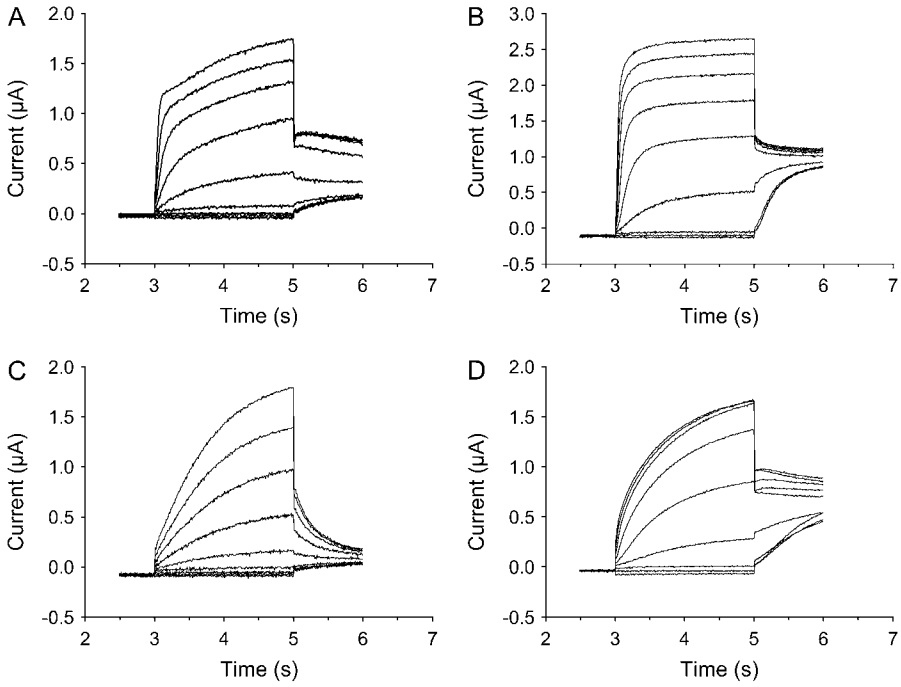


FIGURE 1 Two-electrode voltage-clamp experiments on Kv7.1, 2, 4, and 5 homomeric channels in *Xenopus* oocytes (*A–D*). The channels were activated by voltage steps from $-80$ mV to potentials ranging from $-100$ to $+60$ mV in 20-mV increments (2-s duration), and tail currents were measured at $-30$ mV. Indications of an inactivation process of Kv7.1 and Kv7.5 can be seen by the small hook on the tail current caused by release from inactivation during the initial phase of the 1-s pulse to $-30$ mV as well as the marked difference in activation/deactivation kinetics.

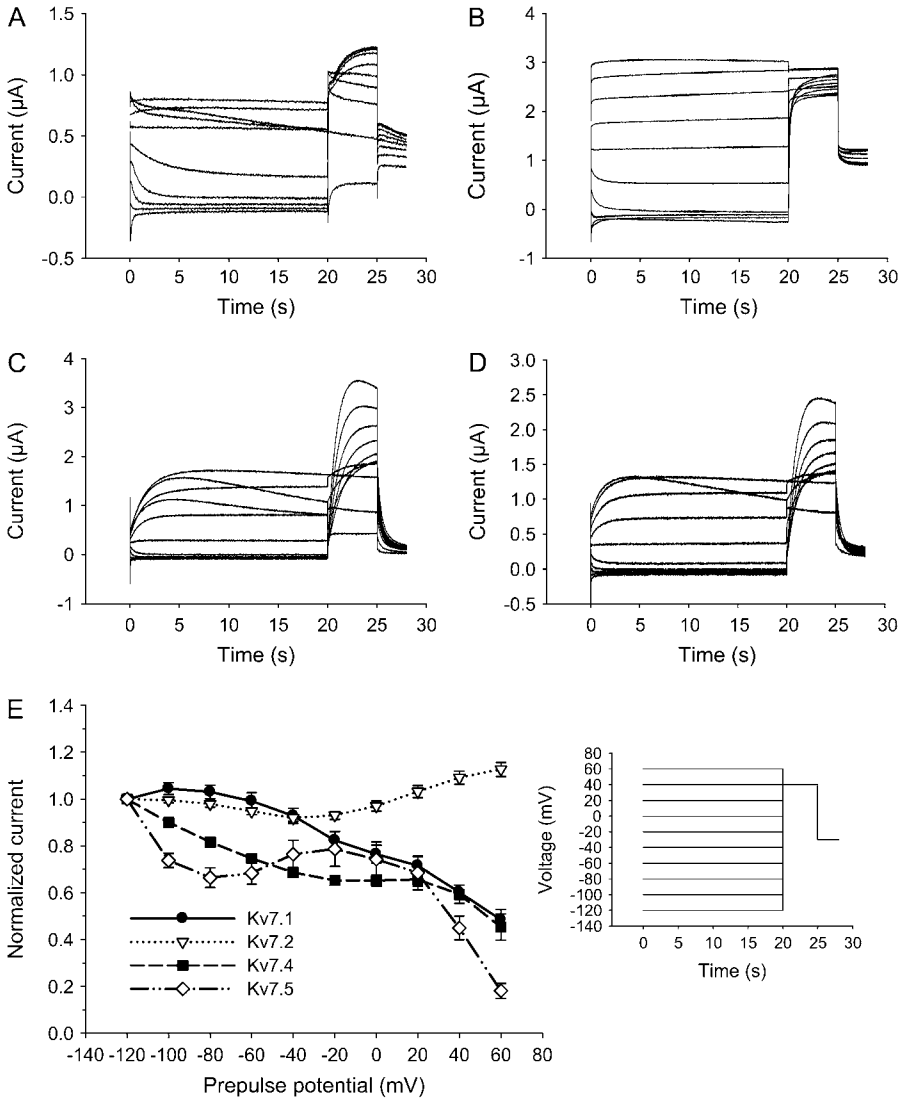


FIGURE 2 Magnitude of inactivation. (*A–D*) The inactivation properties of homomeric Kv7 channel complexes were investigated by voltage-clamp experiments in *Xenopus* oocytes. After a 20-s-long prepulse at potentials ranging from −120 mV to +60 mV ($V_{pre}$), the maximal current amplitudes were measured during a 5-s pulse at +40 mV ($V_{act}$) for each channel subtype: *A*. Kv7.1, *B*. Kv7.2, *C*. Kv7.4, and *D*. Kv7.5 (*inset* shows the voltage protocol). (*E*) The degree of inactivation of each Kv7 channel complex is revealed by plotting the current amplitude normalized to the level measured after a $V_{pre}$ of −120 mV as a function of the preceding $V_{act}$ potential. Maximal inactivation of ~80% is observed for Kv7.5 at +60 mV.

20-s-duration $V_{pre}$ to clamp the cell membrane at holding potentials of −120 mV to +60 mV in 20-mV increments. This step was followed by a $V_{act}$ step to +40 mV. During the 5-s test pulse at +40 mV the noninactivated channels do activate fully, but since they also to some degree inactivate during the test pulse, we use the peak current as a measure of available channels. Due to the channels inactivating during the upstroke of the test current, the protocol may tend to overestimate the degree of inactivation. Plotting the maximal current amplitudes measured during the $V_{act}$ step to +40 mV as a function of the preceding $V_{pre}$ holding potential clearly revealed the steady-state inactivation of homomeric Kv7.1, Kv7.4, and Kv7.5 (Fig. 2, *A–D*). At physiologically relevant potentials, inactivation was most pronounced for Kv7.4 and Kv7.5, which displayed an inactivation of ~30% at $V_{pre} = -50$ mV when compared to $V_{pre} = -120$ mV (Fig. 2 *E*). These experiments demonstrate that in a typical resting neuron ($V_m \sim -70$ mV), significant Kv7 channel inactivation occurs. For the following in-depth investigations, we focused on Kv7.4.

## Onset of inactivation

The onset of inactivation was studied by a three-step protocol consisting of a 10- or 20-s prepulse clamping the cell membrane at −120 mV to recover from inactivation, followed by a step to 0 mV of variable duration (0–28 s in 2-s increments), allowing different degrees of channel inactivation, and finally a 5-s step to +40 mV (Fig. 3 *A*). The time-dependent onset of inactivation is shown by plotting the maximal current amplitude recorded at the $V_{act}$ step to +40 mV as a function of the time spent at 0 mV (Fig. 3 *B*). The results could best be fitted to a three-parameter one-exponential function: $I(x) = A_\infty + A \times \exp(-x/\tau)$, which gave a mean decay time constant, $\tau$, of 9.55 ± 1.14 s, a noninactivation component, $A_\infty$, of 31% ± 2.8%, and a relative amplitude of

the inactivating current, $A$, of 72% ± 3.5%, $n = 7$. To investigate if the 10-s prepulse at −120 mV was long enough to facilitate full recovery from inactivation, we repeated the experiment with a $V_{pre}$ at −120 mV of 20 s. This resulted in a significantly faster inactivation ($\tau$ of 5.06 ± 1.10 s, $n = 3$; $P < 0.05$, Student's $t$-test) and a significantly lower maximal inactivation and amplitude of the exponential ($A_\infty = 48\% \pm 4.3\%$, $P < 0.01$ and $A = 51\% \pm 3.9\%$, $P < 0.05$), indicating that some inactivation must remain even during a 10-s prepulse at −120 mV (Fig. 3 *B*).

## Time-dependent recovery from inactivation

The time-dependent recovery from inactivation of Kv7.4 was studied by a two-step protocol composed of a 20-s-long prepulse at −120 mV followed by a 5-s activation pulse to +40 mV ($V1_{act}$). During this first depolarizing pulse the channels inactivate. To quantify the time needed to recover from inactivation, this pulse was followed by a hyperpolarizing step to −120 mV ranging from 250 ms to 3750 ms in 250-ms increments. The recovery from inactivation is reflected in the current amplitude elicited by a second pulse to +40 mV ($V2_{act}$) (Fig. 4 *A*). A clear time-dependent recovery from inactivation was shown by plotting the current amplitude of $V2_{act}$ in percentage of the preceding $V1_{act}$ maximal current amplitude as a function of the time spent at −120 mV. This could best be fitted to a rising three-parameter one-exponential function with a time constant of 1.47 ± 0.21 s, an $A_0$ of 69.8% ± 2.6%, and an $A$ of 24.8% ± 3.0%, $n = 7$ (Fig. 4 *B*).

## Voltage-dependent recovery from inactivation

Not only increasing time but also increasing hyperpolarizing potentials would be expected to release the inactivation of Kv7.4. We employed a protocol similar to that shown in Fig. 4, but the time between $V1_{act}$ and $V2_{act}$ fixed at 3 s. The variable parameter in this experiment was the holding potential of the intermediate hyperpolarizing step that releases the inactivation, which was clamped at potential ranging from −30 to −120 mV (Fig. 5 *A*). Similar to the time dependence experiments, we plotted the maximal current amplitude of $V2_{act}$ in percentage of the $V1_{act}$ maximal current amplitude but now as a function of the holding potential of the intermediate hyperpolarizing step (Fig. 5 *B*). Fitting these

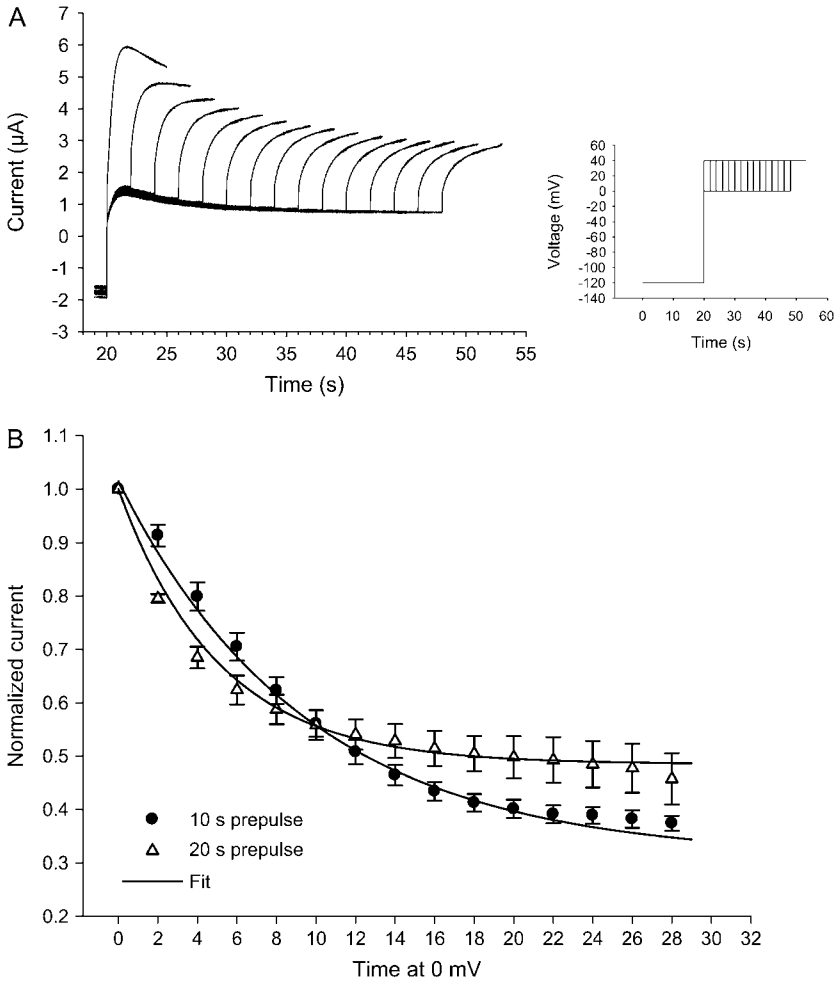


FIGURE 3 Time dependence of inactivation. (*A*) The onset of inactivation of Kv7.4 at 0 mV was studied by a two-step protocol designed to allow the channels to inactivate increasingly. The inset in *B* shows the voltage protocol employed, which clamped the cell membrane at −120 mV for 20 s to allow for recovery from inactivation ($V_{pre}$), followed by a step to 0 mV of 0–28-s duration in 2-s increments. The second step was a depolarizing step to +40 mV for 5 s during which the maximal current amplitude was measured. This experiment was also performed with a 10-s-long $V_{pre}$ (current traces not shown). (*B*) Plotting the maximal current amplitude normalized to the amplitude at $V_{0\ mV,\ 0\ s}$ as a function of the time spent at 0 mV revealed a single-exponential correlation of the onset of inactivation for both protocols. Fitting the data from the two experiments to $I(x) = A_\infty + A \times \exp(-x/\tau)$ gave significantly different time constants: $\tau_{10\ s\ prepulse} = 9.55 \pm 1.14$ s ($n = 7$) and $\tau_{20\ s\ prepulse} = 5.06 \pm 1.10$ s ($n = 3$); $P < 0.05$, $t$-test. The curves are generated from the fitted parameters.

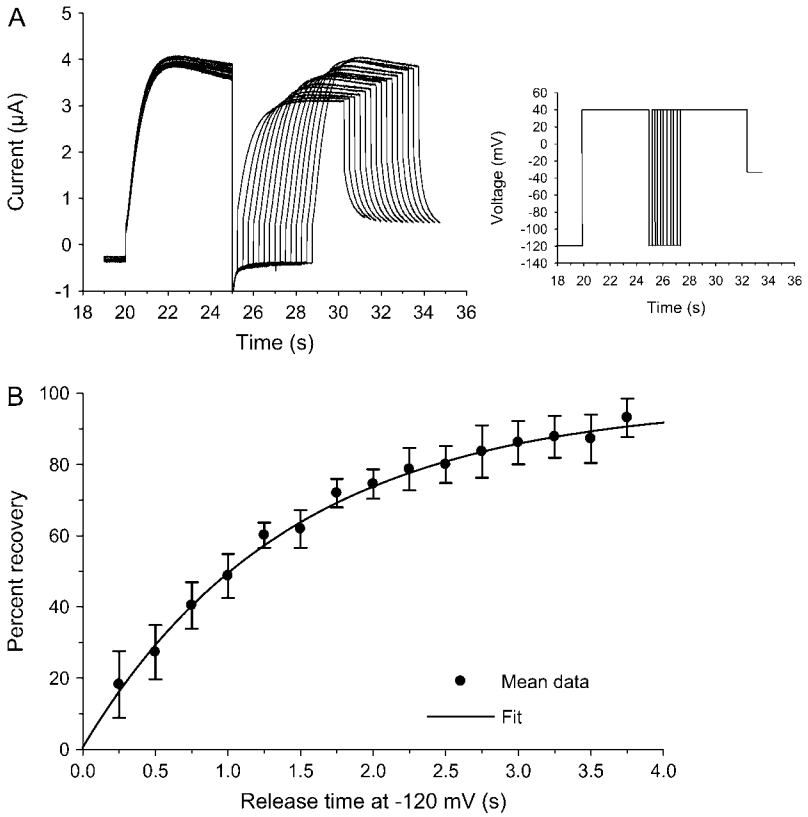


FIGURE 4 Time-dependent recovery from inactivation of Kv7.4. (*A*) The time course of recovery from inactivation was studied by a two-step protocol in which two activating pulses follow a 20-s-long hyperpolarizing pulse at −120 mV. Each +40-mV pulse ($V1_{act}$ and $V2_{act}$) is of 5-s duration, and the variable parameter is the length of the separating −120 mV hyperpolarizing pulse. The duration of the hyperpolarizing pulse ranges from 250 ms to 3750 ms in 250-ms increments (*inset* shows the voltage protocol). (*B*) The maximal current amplitude at $V2_{act}$ is depicted in percentage of the maximal current amplitude at $V1_{act}$ subtracting the $A_0$ (the calculated current amplitude in percentage at time 0) as a function of the release time at −120 mV (i.e., $I[V2_{act}]/I[V1_{act}] \times 100\% - A_0$), and this revealed a single-exponential relationship between the release time and the degree of recovery from inactivation. Fitting the data to $I(x) = A_0 + A \times (1 - \exp(-x/\tau))$ gave a time constant $\tau = 1.47 \pm 0.21$ s ($n = 7$). The curve is generated from the fitted parameters.

data to a three-parameter one-exponential decaying function resulted in a voltage constant of 54.9 ± 3.4 mV, $A_\infty$ = 39.7% ± 3.7%, and $A$ = 6.0% ± 0.88%, $n = 10$ (Fig. 5 *B*).

## Kv7.3 modulates the Kv7.4 inactivation

As Kv7.3 and Kv7.4 can form functionally distinct heteromers (13), we wanted to investigate the inactivation properties of coexpressed Kv7.3 and Kv7.4, and we did this by a protocol comparable to the one shown in Fig. 2 (Fig. 6 *A*). A significant difference in the inactivation properties of homomeric Kv7.4 versus heteromeric Kv7.3+4 channels was evident in the range −40 mV–+60 mV when plotting the maximal current amplitude of the $V_{act}$ step as a function of the $V_{pre}$ potential (Fig. 6 *B*). In contrast to homomeric Kv7.4 channels, which display a flat S-shaped course in the inactivation behavior with no local maximum, heteromeric Kv7.3+4 channels display less inactivation between $V_{pre}$ of −20 mV and +40 mV where the maximal amplitude reaches 89.0% ± 3.5%, $n = 10$ at $V_{pre} = +20$ mV relative to $V_{pre} = -120$ mV (homomeric Kv7.4 amplitude at $V_{pre} = 20$ mV is 65.7% ± 2.8%, $n = 27$ relative to $V_{pre} = -120$).

## Pharmacological modulation of inactivation

A handful of compounds has been used to address the function of Kv7 channels (e.g., retigabine, XE-991, and BMS-204352). The positive modulator retigabine presently undergoing clinical phase III studies has especially been the subject of intense study. It has been shown that retigabine enhances the open probability, shifts the activation curve leftward, and increases the macroscopic current of Kv7 channels (16,41–44). However, none of these studies has investigated the effect on the inactivation of Kv7.4. To address this we employed the standard inactivation voltage protocol, as used in Figs. 2 and 6, in the absence and presence of 10 μM retigabine (Fig. 7, *A* and *B*). The two curves describing the measured currents at each potential normalized to the control current at −120 mV and plotted as a function of $V_{pre}$ were parallel over the range of $V_{pre}$ tested (−120 mV–+80 mV) (Fig. 7 *E*). When plotting the retigabine-induced current relative to the control current at each potential the modulation of inactivation by retigabine was also minor (the potentiation ranged from 170% ± 15% at a $V_{pre}$ of −120 mV to 269% ± 50% at a $V_{pre}$ of +80 mV, $n = 7$). We quantified this as the slope of the best linear fit to the percentage of control data, which was calculated as $\alpha_{RTG}$ = 0.33% ± 0.21%/mV, $n = 7$ (Fig. 7, *E–G*).

In a similar manner we tested if the inhibitory effect of XE-991 was related to a changed inactivation. Hence, 100 μM XE-991 was applied as described above, and the rate of inactivation of Kv7.4 was compared before and after drug application (Fig. 7, *A* and *D*). As with retigabine, the maximal current amplitude relative to control conditions over the range of $V_{pre}$ tested was close to parallel and in the range of 40%–45% (45% ± 4.3% at $V_{pre} = -120$ mV to

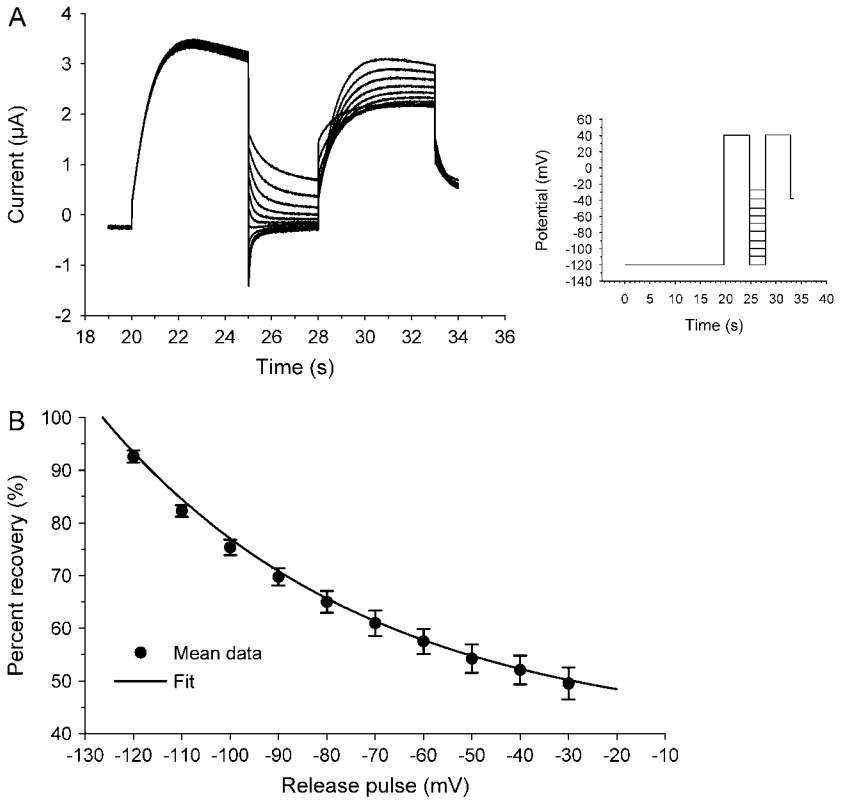


FIGURE 5 Voltage-dependent recovery from inactivation of Kv7.4. (*A*) The kinetics of recovery from inactivation was studied by a two-step protocol similar to the one used in the time-dependent recovery experiments, but with the duration of the release pulse fixed at 3 s. The variable in this experiment was the voltage employed to clamp the membrane during the release pulse, which ranged from −120 mV to −30 mV in 10-mV increments (*inset* shows the protocol). (*B*) The maximal current amplitude recorded at $V2_{act}$ in percentage of the corresponding amplitude of $V1_{act}$ plotted as a function of the holding potential of the release pulse could best be fitted to a single-exponential function: $I(x) = A_\infty + A \times \exp(-x/\tau)$, resulting in a voltage-constant $\tau = 54.9 \pm 3.4$ mV ($n = 10$).

45% ± 8.6% at $V_{pre} = +80$ mV, $n = 5$). The slope of the best linear fit was calculated to $\alpha_{XE\text{-}991} = -0.016\% \pm 0.017\%$/mV, $n = 5$ (Fig. 7, *E–G*).

BMS-204352 was originally developed for the treatment of stroke, and the mechanism was thought to be by opening BK channels (45). However, it has also been shown to be a potent activator of Kv7 channels (41,46,47). A detailed characterization of the mode of action on the Kv7 channels has not yet been described, so we investigated the effect of BMS-204352 on the inactivation properties of Kv7.4. A total of 10 μM BMS-204352 potentiated the current to 690% ± 106%, $n = 5$ of control measured at the end of a depolarizing step during the following repeated voltage protocol: 4 s at −80 mV, 2 s at +40 mV, and 1 s at −30 mV (not shown). In contrast to retigabine and XE-991, a clear effect on inactivation was observed with BMS-204352 (Fig. 7, *A* and *C*). The maximal $V_{act}$ current amplitude increased over the range of $V_{pre}$ tested from 578% ± 15% of control at $V_{pre} = -120$ mV to 1745% ± 422% at $V_{pre} = +80$ mV, $n = 3$. The slope of the best linear fit of the percentage of control data reflects abolishment of Kv7.4 inactivation by BMS-204352, as it was calculated to $\alpha_{BMS} = 5.24\% \pm 1.51\%$/mV, $n = 3$ (Fig. 7, *E–G*).

## DISCUSSION

The nonneuronal Kv7.1 potassium channel has been described to inactivate (38,39,48), whereas the general notion has been that the other Kv7 family members do not inactivate. Contrary to this general view on the biophysical properties of the neuronal Kv7 channels, we here show that Kv7.4 and Kv7.5 channels indeed do inactivate. We have performed detailed studies on Kv7.4 showing that the macroscopic inactivation is voltage dependent and is augmented as a function of increased holding potentials, reaching a maximum >60% at +80 mV. Kv7.4, as well as Kv7.5 channels, was found to inactivate to a larger extent than Kv7.1.

The kinetics of Kv7.4 channel inactivation is slow, with time constants of 5–10 s depending on the duration of the preceding hyperpolarizing pulse ($\tau_{10\ s\ prepulse} = 9.55 \pm 1.14$ s and $\tau_{20\ s\ prepulse} = 5.06 \pm 1.10$ s). Recovery from inactivation of Kv7.4 is both time and voltage dependent. When inactivation was released by hyperpolarizing pulses at −120 mV at increasing time intervals, the recovery from inactivation was clearly time dependent with a time constant of 1.47 ± 0.21 s. The inactivation kinetics of Kv7.4 is apparently much slower than that of Kv7.1, as Tristani-Firouzi and Sanguinetti found that Kv7.1 inactivates monoexponentially at +20 mV with a time constant of 130 ms after an initial delay of ~75 ms (38). The time constants for recovery from inactivation of Kv7.1 was likewise much faster, ranging from 30–40 ms and showing very little voltage dependence at voltages ranging from −90 to −30 mV (38). However, since the kinetics of inactivation and recovery from inactivation in their study was determined from the hooked tail current, they may only reflect the early phase of both

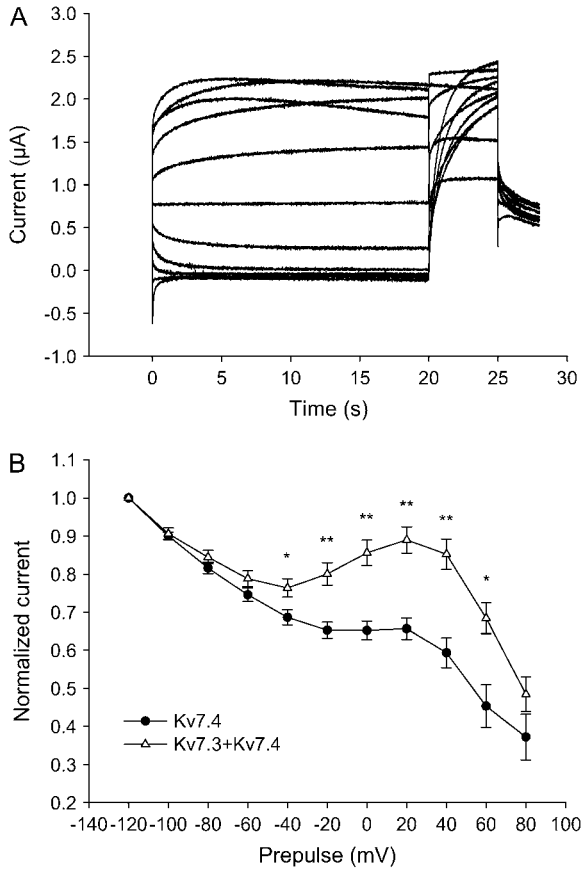


FIGURE 6 Kv7.3+4 heteromers inactivate differently from Kv7.4 homomers. (*A*) Cells expressing heteromeric Kv7.3+4 channels were investigated for the inactivation behavior of the respective channels with the same voltage protocol as in Fig. 2 (expanded to include a prepulse step to +80 mV). (*B*) The figure shows the normalized maximal current recorded at a 5-s-long depolarizing pulse to +40 mV preceded by a 20-s-long prepulse ($V_{pre}$) ranging from −120 mV to +80 mV in 20-mV increments for both Kv7.4 and Kv7.3 + 4. Current amplitudes are plotted as a function of the holding potential during the 20-s-long prepulse, and the two channel complexes are significantly different in this respect after a prepulse ranging from −40 mV to +60 mV. Asterisks indicate the level of significance (*, $P < 0.05$; **, $P < 0.005$, *t*-test, $n = 10$ and 27, Kv7.3 + 4 and Kv7.4, respectively).

phenomena. The degree of Kv7.1 inactivation in both studies was found to be ~35% at +40 mV with a similar voltage dependence despite the different protocols used to reflect the inactivation.

It has been demonstrated that Kv7.3 and Kv7.4 can form functional heteromers (13), so we investigated if such complexes had an inactivation profile different from Kv7.4 homomers. The quantity of inactivated heteromers was significantly decreased at potentials from −40 mV to + 60 mV. This indicates that more active Kv7.3 + Kv7.4 channel complexes will be present at these potentials relative to homomeric Kv7.4 channels.

In a final investigation we addressed if different Kv7 channel modulators had any impact on the inactivation properties of the channels. It was demonstrated that the Kv7.4 channel activator retigabine and the inhibitor XE-991 did not mediate their effects through changed inactivation. In contrast, BMS-204352 abolished the inactivation of Kv7.4 channels. These data demonstrate that the Kv7 openers retigabine and BMS-204352 have distinct modes of action.

It is known from Kv7.1 inactivation that this can be abolished by coexpression with KCNE1 (minK), which is in agreement with the notion that the endogenous $I_{Ks}$ current does not inactivate (38). It has been suggested that this modification of the channel kinetics is accomplished by the C-terminus of KCNE1 protruding into the Kv7.1 complex and binding to the pore loop (49). The modest effect of Kv7.3 and retigabine as opposed to the strong effect of BMS-204352 on Kv7.4 inactivation may likewise be caused by the physical interaction resulting in an allosteric modulation of the channel complex. However, we do not know the specific binding sites of these molecules to the Kv7.4 complex. It is likely that BMS-204352 binds to a site other than retigabine, since they are structurally quite different molecules. Further, the two compounds modify the Kv7 channel subtypes differentially since BMS-203352 blocks Kv7.1 whereas retigabine shows no effect on this channel (44,50). Likewise, the drugs show differential effects on the neuronal Kv7 channels (51).

One of the ways a drug can activate an ion channel is by removing its inactivation, as is the case for BMS-204352. The effects of BMS-204352 is, however, significantly larger than what can be accounted for by reduced inactivation alone (Fig. 7). The compound also activates the Kv7.4 channel by shifting the voltage-dependent activation curve toward negative values (50) as well as by activating a voltage-independent Kv7.4 current (41). Since the open probability of Kv7.4 channels at positive membrane potentials is only ~0.18 (52), there is room for an increased opening of the channel in the presence of compound, which must also occur for the current to increase by more than fivefold at the noninactivation potential of −120 mV.

In this study Kv7.4 and Kv7.5 are found to inactivate to the largest degree, whereas Kv7.2 does not inactivate. Kv7.4 and Kv7.5 exhibit a number of similar characteristics in contrast to Kv7.2: Kv7.4 has a greater amino acid sequence homology with Kv7.5 than with Kv7.2; pharmacologically BMS-204352 activates Kv7.4 and Kv7.5, whereas it does not modify Kv7.2/3 (50); biophysically the unitary currents of Kv7.4 and Kv7.5 are 2.1 and 2.2 pS, whereas that of Kv7.2 is 6.2 pS (52,53); the maximal open probability of Kv7.4 and Kv7.5 are 0.18 and 0.17, respectively, whereas it is 0.07 for Kv7.2. This does not in itself explain why Kv7.4 and Kv7.5 inactivate and Kv7.2 does not, and to address this question it is important to study the residues in the Kv7 channels involved in the inactivation process of which we currently have no clear indication.

This study shows that Kv7.4 channel inactivation is different from classical N- and C-type inactivation found in

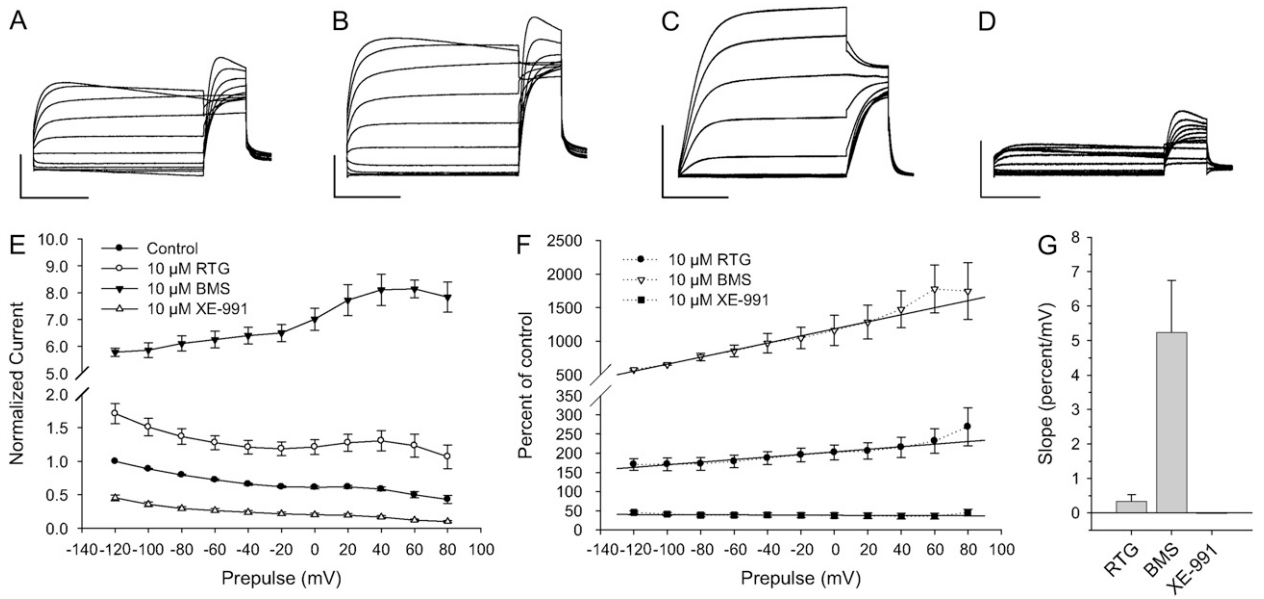


FIGURE 7 Pharmacological modulation of Kv7.4 inactivation. (*A–D*) Two-electrode voltage-clamp experiments on three different oocytes under control conditions (*A*) and after application of 10 $\mu$M retigabine (RTG; *B*), 10 $\mu$M BMS-204352 (*C*), and 100 $\mu$M XE-991 (*D*). The voltage protocol consist of a 20-s-long prepulse ($V_{pre}$) ranging from −120 mV to +80 mV in 20-mV increments, followed by a depolarizing step to +40 mV ($V_{act}$) and ended by a 1-s step to −30 mV. The scale bars are for control and RTG traces 3 $\mu$A and 5 s, for the BMS experiment 6 $\mu$A and 5 s, and for XE-991 1 $\mu$A and 5 s. (*E*) Plot showing the normalized current levels before and after application of RTG, BMS, and XE-991, respectively. (*F*) Graphs illustrate the best linear fit of the measured current expressed as percentage of control data. Best-fit slope values are (in percentage per mV) $\alpha_{RTG} = 0.33 \pm 0.21$ ($n = 7$), $\alpha_{XE\text{-}991} = -0.016 \pm 0.017$ ($n = 5$), and $\alpha_{BMS} = 5.24 \pm 1.51$ ($n = 3$). (*G*) Histogram illustrating the differences between the slope values determined for RTG, BMS, and XE-991.

voltage-gated $Na^+$ channels and voltage-gated $K^+$ channels of the *Shaker* type (38,48,54–57). Features that distinguish Kv7.4 inactivation from N- and C-type inactivation are slow onset and voltage dependency. This is also true for Kv7.1 inactivation (38), suggesting that the inactivation mechanism for these two Kv7 channel subtypes are similar.

The inactivation property may have important bearings for the pathophysiology and pharmacology of the neuronal Kv7 channels. Within the family of Kv7 channels, inactivation at physiologically relevant potentials was most prominent for Kv7.4 and Kv7.5 channels. Of the five Kv7 channel subunits, Kv7.4 displays the most restricted expression pattern, being present in the inner ear and the auditory pathways of the brain but also in certain dopaminergic neurones (58,59). Hence, Kv7.4 channels could represent a particularly relevant target for treatment with drugs specifically activating the Kv7.4 channel as efficacy, and side effect profiles of such a compound could prove superior to panreactive compounds affecting all neuronal members of the Kv7 family.

In conclusion we have described inactivation as a new regulatory mechanism for Kv7.4 and Kv7.5 channels. At physiologically relevant resting potentials, the current is reduced by more than 30% due to steady-state inactivation. These results add to a more profound understanding of the biophysical nature of the Kv7 channel family and their physiological impact. Pharmacological channel modulators influence the inactivation properties differentially, so this newly discovered regulatory mechanism is of further importance when developing drugs targeted for these channels. Physiological signaling molecules may also influence the steady-state inactivation of Kv7 channels, and if this proves to be the case it will be an efficient way of modulating neuronal excitability.

Prof. Thomas Jentsch is acknowledged for kindly supplying human Kv7.2, 3, and 4 cDNA and Prof. Michel Lazdunski for supplying Kv7.1 cDNA.

This work was supported by the Danish National Research Foundation and the Danish Medical Research Council (to S.P.O.).

## REFERENCES

1. Robbins, J. 2001. KCNQ potassium channels: physiology, pathophysiology, and pharmacology. *Pharmacol. Ther.* 90:1–19.
2. Jentsch, T. J. 2000. Neuronal KCNQ potassium channels: physiology and role in disease. *Nat. Rev. Neurosci.* 1:21–30.
3. Jespersen, T., M. Grunnet, and S. P. Olesen. 2005. The KCNQ1 potassium channel: from gene to physiological function. *Physiology (Bethesda).* 20:408–416.
4. Wang, Q., M. E. Curran, I. Splawski, T. C. Burn, J. M. Millholland, T. J. VanRaay, J. Shen, K. W. Timothy, G. M. Vincent, T. de Jager, P. J. Schwartz, J. A. Toubin, A. J. Moss, D. L. Atkinson, G. M. Landes, T. D. Connors, and M. T. Keating. 1996. Positional cloning of a novel potassium channel gene: KVLQT1 mutations cause cardiac arrhythmias. *Nat. Genet.* 12:17–23.
5. Sanguinetti, M. C., M. E. Curran, A. Zou, J. Shen, P. S. Spector, D. L. Atkinson, and M. T. Keating. 1996. Coassembly of K(V)LQT1 and minK (IsK) proteins to form cardiac I(Ks) potassium channel. *Nature.* 384:80–83.

6. Barhanin, J., F. Lesage, E. Guillemare, M. Fink, M. Lazdunski, and G. Romey. 1996. K(V)LQT1 and lsK (minK) proteins associate to form the I(Ks) cardiac potassium current. *Nature*. 384:78–80.
7. Brown, D. A., and P. R. Adams. 1980. Muscarinic suppression of a novel voltage-sensitive K+ current in a vertebrate neurone. *Nature*. 283:673–676.
8. Biervert, C., B. C. Schroeder, C. Kubisch, S. F. Berkovic, P. Propping, T. J. Jentsch, and O. K. Steinlein. 1998. A potassium channel mutation in neonatal human epilepsy. *Science*. 279:403–406.
9. Singh, N. A., C. Charlier, D. Stauffer, B. R. DuPont, R. J. Leach, R. Melis, G. M. Ronen, I. Bjerre, T. Quattlebaum, J. V. Murphy, M. L. McHarg, D. Gagnon, T. O. Rosales, A. Peiffer, V. E. Anderson, and M. Leppert. 1998. A novel potassium channel gene, KCNQ2, is mutated in an inherited epilepsy of newborns. *Nat. Genet.* 18:25–29.
10. Charlier, C., N. A. Singh, S. G. Ryan, T. B. Lewis, B. E. Reus, R. J. Leach, and M. Leppert. 1998. A pore mutation in a novel KQT-like potassium channel gene in an idiopathic epilepsy family. *Nat. Genet.* 18:53–55.
11. Wang, H. S., Z. Pan, W. Shi, B. S. Brown, R. S. Wymore, I. S. Cohen, J. E. Dixon, and D. McKinnon. 1998. KCNQ2 and KCNQ3 potassium channel subunits: molecular correlates of the M-channel. *Science*. 282: 1890–1893.
12. Schroeder, B. C., C. Kubisch, V. Stein, and T. J. Jentsch. 1998. Moderate loss of function of cyclic-AMP-modulated KCNQ2/KCNQ3 K+ channels causes epilepsy. *Nature (Lond.)*. 396:687–690.
13. Kubisch, C., B. C. Schroeder, T. Friedrich, B. Lutjohann, A. El Amraoui, S. Marlin, C. Petit, and T. J. Jentsch. 1999. KCNQ4, a novel potassium channel expressed in sensory outer hair cells, is mutated in dominant deafness. *Cell (Cambridge, Massachusetts)*. 96:437–446.
14. Coucke, P. J., P. Van Hauwe, P. M. Kelley, H. Kunst, I. Schatteman, D. Van Velzen, J. Meyers, R. J. Ensink, M. Verstreken, F. Declau, H. Marres, K. Kastury, S. Bhasin, W. T. McGuirt, R. J. H. Smith, C. W. R. J. Cremers, P. Van de Heyning, P. J. Willems, S. D. Smith, and G. Van Camp. 1999. Mutations in the KCNQ4 gene are responsible for autosomal dominant deafness in four DFNA2 families. *Hum. Mol. Genet.* 8:1321–1328.
15. Talebizadeh, Z., P. M. Kelley, J. W. Askew, K. W. Beisel, and S. D. Smith. 1999. Novel mutation in the KCNQ4 gene in a large kindred with dominant progressive hearing loss. *Hum. Mutat.* 14:493–501.
16. Jensen, H. S., K. Callo, T. Jespersen, B. S. Jensen, and S. P. Olesen. 2005. The KCNQ5 potassium channel from mouse: a broadly expressed M-current like potassium channel modulated by zinc, pH, and volume changes. *Brain Res. Mol. Brain Res.* 139:52–62.
17. Schroeder, B. C., M. Hechenberger, F. Weinreich, C. Kubisch, and T. J. Jentsch. 2000. KCNQ5, a novel potassium channel broadly expressed in brain, mediates M-type currents. *J. Biol. Chem.* 275:24089–24095.
18. Lerche, C., C. R. Scherer, G. Seebohm, C. Derst, A. D. Wei, A. E. Busch, and K. Steinmeyer. 2000. Molecular cloning and functional expression of KCNQ5, a potassium channel subunit that may contribute to neuronal M-current diversity. *J. Biol. Chem.* 275:22395–22400.
19. Grunnet, M., T. Jespersen, N. MacAulay, N. K. Jorgensen, N. Schmitt, O. Pongs, S. P. Olesen, and D. A. Klaerke. 2003. KCNQ1 channels sense small changes in cell volume. *J. Physiol.* 549:419–427.
20. Marx, S. O., J. Kurokawa, S. Reiken, H. Motoike, J. D′Armiento, A. R. Marks, and R. S. Kass. 2002. Requirement of a macromolecular signaling complex for beta adrenergic receptor modulation of the KCNQ1-KCNE1 potassium channel. *Science*. 295:496–499.
21. Potet, F., J. D. Scott, R. Mohammad-Panah, D. Escande, and I. Baro. 2001. AKAP proteins anchor cAMP-dependent protein kinase to KvLQT1/IsK channel complex. *Am. J. Physiol. Heart Circ. Physiol.* 280:H2038–H2045.
22. Loussouarn, G., K. H. Park, C. Bellocq, I. Baro, F. Charpentier, and D. Escande. 2003. Phosphatidylinositol-4,5-bisphosphate, PIP2, controls KCNQ1/KCNE1 voltage-gated potassium channels: a functional homology between voltage-gated and inward rectifier K+ channels. *EMBO J.* 22:5412–5421.
23. Peretz, A., H. Schottelndreier, L. B. Aharon-Shamgar, and B. Attali. 2002. Modulation of homomeric and heteromeric KCNQ1 channels by external acidification. *J. Physiol.* 545:751–766.
24. Unsold, B., G. Kerst, H. Brousos, M. Hubner, R. Schreiber, R. Nitschke, R. Greger, and M. Bleich. 2000. KCNE1 reverses the response of the human K+ channel KCNQ1 to cytosolic pH changes and alters its pharmacology and sensitivity to temperature. *Pflugers Arch.* 441:368–378.
25. Tinel, N., S. Diochot, M. Borsotto, M. Lazdunski, and J. Barhanin. 2000. KCNE2 confers background current characteristics to the cardiac KCNQ1 potassium channel. *EMBO J.* 19:6326–6330.
26. Schroeder, B. C., S. Waldegger, S. Fehr, M. Bleich, R. Warth, R. Greger, and T. J. Jentsch. 2000. A constitutively open potassium channel formed by KCNQ1 and KCNE3. *Nature*. 403:196–199.
27. Grunnet, M., T. Jespersen, H. B. Rasmussen, T. Ljungstrom, N. K. Jorgensen, S. P. Olesen, and D. A. Klaerke. 2002. KCNE4 is an inhibitory subunit to the KCNQ1 channel. *J. Physiol.* 542:119–130.
28. Angelo, K., T. Jespersen, M. Grunnet, M. S. Nielsen, D. A. Klaerke, and S. P. Olesen. 2002. KCNE5 induces time- and voltage-dependent modulation of the KCNQ1 current. *Biophys. J.* 83:1997–2006.
29. Shapiro, M. S., J. P. Roche, E. J. Kaftan, H. Cruzblanca, K. Mackie, and B. Hille. 2000. Reconstitution of muscarinic modulation of the KCNQ2/KCNQ3 K(+) channels that underlie the neuronal M current. *J. Neurosci.* 20:1710–1721.
30. Simmons, M. A., C. R. Schneider, and J. E. Krause. 1994. Regulation of the responses to gonadotropin-releasing hormone, muscarine and substance P in sympathetic neurons by changes in cellular constituents and intracellular application of peptide fragments of the substance P receptor. *J. Pharmacol. Exp. Ther.* 271:581–589.
31. Cruzblanca, H., D. S. Koh, and B. Hille. 1998. Bradykinin inhibits M current via phospholipase C and Ca2+ release from IP3-sensitive Ca2+ stores in rat sympathetic neurons. *Proc. Natl. Acad. Sci. USA*. 95:7151–7156.
32. Suh, B. C., and B. Hille. 2002. Recovery from muscarinic modulation of M current channels requires phosphatidylinositol 4,5-bisphosphate synthesis. *Neuron*. 35:507–520.
33. Zhang, H., L. C. Craciun, T. Mirshahi, T. Rohacs, C. M. Lopes, T. Jin, and D. E. Logothetis. 2003. PIP(2) activates KCNQ channels, and its hydrolysis underlies receptor-mediated inhibition of M currents. *Neuron*. 37:963–975.
34. Ford, C. P., P. L. Stemkowski, P. E. Light, and P. A. Smith. 2003. Experiments to test the role of phosphatidylinositol 4,5-bisphosphate in neurotransmitter-induced M-channel closure in bullfrog sympathetic neurons. *J. Neurosci.* 23:4931–4941.
35. Delmas, P., and D. A. Brown. 2005. Pathways modulating neural KCNQ/M (Kv7) potassium channels. *Nat. Rev. Neurosci.* 6:850–862.
36. Hougaard, C., D. A. Klaerke, E. K. Hoffmann, S. P. Olesen, and N. K. Jorgensen. 2004. Modulation of KCNQ4 channel activity by changes in cell volume. *Biochim. Biophys. Acta*. 1660:1–6.
37. Seebohm, G., N. Strutz-Seebohm, R. Baltaev, G. Korniychuk, M. Knirsch, J. Engel, and F. Lang. 2005. Regulation of KCNQ4 potassium channel prepulse dependence and current amplitude by SGK1 in Xenopus oocytes. *Cell. Physiol. Biochem.* 16:255–262.
38. Tristani-Firouzi, M., and M. C. Sanguinetti. 1998. Voltage-dependent inactivation of the human K+ channel KvLQT1 is eliminated by association with minimal K+ channel (minK) subunits. *J. Physiol.* 510:37–45.
39. Seebohm, G., C. R. Scherer, A. E. Busch, and C. Lerche. 2001. Identification of specific pore residues mediating KCNQ1 inactivation. A novel mechanism for long QT syndrome. *J. Biol. Chem.* 276:13600–13605.
40. Grunnet, M., S. P. Olesen, D. A. Klaerke, and T. Jespersen. 2005. hKCNE4 inhibits the hKCNQ1 potassium current without affecting the activation kinetics. *Biochem. Biophys. Res. Commun.* 328:1146–1153.
41. Schroder, R. L., D. Strobaek, S. P. Olesen, and P. Christophersen. 2003. Voltage-independent KCNQ4 currents induced by (±)BMS-204352. *Pflugers Arch.* 446:607–616.

42. Bentzen, B. H., N. Schmitt, K. Calloe, B. W. Dalby, M. Grunnet, and S. P. Olesen. 2006. The acrylamide (S)-1 differentially affects Kv7 (KCNQ) potassium channels. *Neuropharmacology.* 51:1068–1077.

43. Tatulian, L., and D. A. Brown. 2003. Effect of the KCNQ potassium channel opener retigabine on single KCNQ2/3 channels expressed in CHO cells. *J. Physiol.* 549:57–63.

44. Tatulian, L., P. Delmas, F. C. Abogadie, and D. A. Brown. 2001. Activation of expressed KCNQ potassium currents and native neuronal M-type potassium currents by the anti-convulsant drug retigabine. *J. Neurosci.* 21:5535–5545.

45. Gribkoff, V. K., J. E. Starrett Jr., S. I. Dworetzky, P. Hewawasam, C. G. Boissard, D. A. Cook, S. W. Frantz, K. Heman, J. R. Hibbard, K. Huston, G. Johnson, B. S. Krishnan, G. G. Kinney, L. A. Lombardo, N. A. Meanwell, P. B. Molinoff, R. A. Myers, S. L. Moon, A. Ortiz, L. Pajor, R. L. Pieschl, D. J. Post-Munson, L. J. Signor, N. Srinivas, M. T. Taber, G. Thalody, J. T. Trojnacki, H. Wiener, K. Yeleswaram, and S. W. Yeola. 2001. Targeting acute ischemic stroke with a calcium-sensitive opener of maxi-K potassium channels. *Nat. Med.* 7: 471–477.

46. Dupuis, D. S., R. L. Schroder, T. Jespersen, J. K. Christensen, P. Christophersen, B. S. Jensen, and S. P. Olesen. 2002. Activation of KCNQ5 channels stably expressed in HEK293 cells by BMS-204352. *Eur. J. Pharmacol.* 437:129–137.

47. Schroder, R. L., T. Jespersen, P. Christophersen, D. Strobaek, B. S. Jensen, and S. P. Olesen. 2001. KCNQ4 channel activation by BMS-204352 and retigabine. *Neuropharmacology.* 40:888–898.

48. Pusch, M., R. Magrassi, B. Wollnik, and F. Conti. 1998. Activation and inactivation of homomeric KvLQT1 potassium channels. *Biophys. J.* 75:785–792.

49. Romey, G., B. Attali, C. Chouabe, I. Abitbol, E. Guillemare, J. Barhanin, and M. Lazdunski. 1997. Molecular mechanism and functional significance of the MinK control of the KvLQT1 channel activity. *J. Biol. Chem.* 272:16713–16716.

50. Korsgaard, M. P., B. P. Hartz, W. D. Brown, P. K. Ahring, D. Strobaek, and N. R. Mirza. 2005. Anxiolytic effects of Maxipost (BMS-204352) and retigabine via activation of neuronal Kv7 channels. *J. Pharmacol. Exp. Ther.* 314:282–292.

51. Dalby-Brown, W., H. H. Hansen, M. P. Korsgaard, N. Mirza, and S. P. Olesen. 2006. K(v)7 channels: function, pharmacology and channel modulators. *Curr. Top. Med. Chem.* 6:999–1023.

52. Li, Y., N. Gamper, and M. S. Shapiro. 2004. Single-channel analysis of KCNQ K+ channels reveals the mechanism of augmentation by a cysteine-modifying reagent. *J. Neurosci.* 24:5079–5090.

53. Selyanko, A. A., J. K. Hadley, and D. A. Brown. 2001. Properties of single M-type KCNQ2/KCNQ3 potassium channels expressed in mammalian cells. *J. Physiol.* 534:15–24.

54. Roux, M. J., R. Olcese, L. Toro, F. Bezanilla, and E. Stefani. 1998. Fast inactivation in Shaker K+ channels. Properties of ionic and gating currents. *J. Gen. Physiol.* 111:625–638.

55. Hoshi, T., W. N. Zagotta, and R. W. Aldrich. 1990. Biophysical and molecular mechanisms of Shaker potassium channel inactivation. *Science.* 250:533–538.

56. Rettig, J., S. H. Heinemann, F. Wunder, C. Lorra, D. N. Parcej, J. O. Dolly, and O. Pongs. 1994. Inactivation properties of voltage-gated K+ channels altered by presence of beta-subunit. *Nature.* 369:289–294.

57. Liu, Y., M. E. Jurman, and G. Yellen. 1996. Dynamic rearrangement of the outer mouth of a K+ channel during gating. *Neuron.* 16:859–867.

58. Hansen, H. H., C. Ebbesen, C. Mathiesen, P. Weikop, L. C. Ronn, O. Waroux, J. Scuvee-Moreau, V. Seutin, and J. D. Mikkelsen. 2006. The KCNQ channel opener retigabine inhibits the activity of mesencephalic dopaminergic systems of the rat. *J. Pharmacol. Exp. Ther.* 318:1006–1019.

59. Kharkovets, T., J. P. Hardelin, S. Safieddine, M. Schweizer, A. El Amraoui, C. Petit, and T. J. Jentsch. 2000. KCNQ4, a K+ channel mutated in a form of dominant deafness, is expressed in the inner ear and the central auditory pathway. *Proc. Natl. Acad. Sci. USA.* 97:4333–4338.